

Compatibility of phenomenological dipole cross sections with the Balitsky-Kovchegov equation

Daniël Boer,^{*} Andre Utermann,[†] and Erik Wessels[‡]
*Department of Physics and Astronomy, Vrije Universiteit Amsterdam,
 De Boelelaan 1081, 1081 HV Amsterdam, The Netherlands*

Phenomenological models of the dipole cross section that enters in the description of for instance deep inelastic scattering at very high energies have had considerable success in describing the available small- x data in both the saturation region and the so-called extended geometric scaling (EGS) region. We investigate to what extent such models are compatible with the numerical solutions of the Balitsky-Kovchegov (BK) equation which is expected to describe the nonlinear evolution in x of the dipole cross section in these momentum regions. We find that in the EGS region the BK equation yields results that are qualitatively different from those of phenomenological studies. In particular, geometric scaling around the saturation scale is only obtained at asymptotic rapidities. We find that in this limit, the anomalous dimension $\gamma(r, x)$ of phenomenological models approaches a limiting function that is universal for a large range of initial conditions. At the saturation scale, this function equals approximately 0.44, in contrast to the value 0.628 commonly used in the models. We further investigate the dependence of these results on the starting distribution, the small- r limit of the anomalous dimension for fixed rapidities and the x -dependence of the saturation scale.

PACS numbers: 12.38.-t, 13.60.Hb, 11.80.La, 11.10.Hi

I. INTRODUCTION

At very high energy, deep inelastic scattering (DIS) of a virtual photon off a proton can be described as the scattering of a color dipole off small- x partons, predominantly gluons, in the proton [1]. The evolution in x of the corresponding dipole cross section has been the subject of many investigations. The earliest and best-known equation describing x -evolution at high energy, i.e. small values of x , is the BFKL equation [2, 3]. It is a linear evolution equation based on resummation of logarithms in $1/x$, which are dominant at small x . The BFKL equation predicts an exponential growth of the dipole cross section as x decreases, which potentially violates unitarity. Attempts to solve this problem have resulted in the formulation of a variety of nonlinear evolution equations, the earliest example of which is the GLR equation [4, 5] for the gluon distribution. More recently, a nonlinear evolution equation for the dipole cross section has been obtained, the Balitsky-Kovchegov (BK) equation [6, 7]. As a consequence of the nonlinearity, the dipole cross section saturates with decreasing x , thereby offering a resolution to the unitarity problem arising from the BFKL equation.

The momentum scale at which nonlinearity becomes important and saturation sets in is called the saturation scale Q_s . This scale grows as x decreases, which means that if Q_s becomes larger than 1 GeV say, the coupling constant at Q_s will be small enough for small coupling methods to become applicable. In spite of this, even for the simplest nonlinear evolution equation –the BK equation– analytical solutions have been found in specific cases only [8, 9, 10, 11, 12, 13, 14]. However, numerical solutions to the BK equation have been obtained in all momentum regions [15, 16, 17, 18, 19, 20, 21, 22]. For a review of the properties of the numerical solutions cf. [23].

In the absence of exact solutions of the nonlinear evolution equations, the dipole cross section has been modeled using both theoretical considerations and experimental data. In the saturation region, such models have been derived theoretically on the basis of multiple rescattering of the dipole off the target, to various levels of sophistication. In what is now commonly referred to as the Color Glass Condensate (CGC) formalism [24, 25], the small- x gluons are described as a color field generated by the large- x partons, which act as static sources.

^{*}Electronic address: D.Boer@few.vu.nl

[†]Electronic address: A.Utermann@few.vu.nl

[‡]Electronic address: E.Wessels@few.vu.nl

Scattering amplitudes are expressed as two-point functions of lightlike Wilson lines that are averaged over the possible source configurations, which evolve with x . The averaged two-point functions satisfy a tower of nonlinear evolution equations, the Balitsky-JIMWLK equations [26], coupling them to ever higher n -point functions. However, in a mean field approximation the Balitsky-JIMWLK equations reduce to a single evolution equation, the BK equation. The saturated state of high-gluon density at small x described by the CGC has been under very active theoretical and experimental investigation in recent years. Valuable further tests will be provided by future colliders that are able to probe well into the saturation region, such as the LHC and a possible electron-ion collider.

The phenomenological models for the dipole cross section that are used to investigate the available HERA and RHIC data are constructed on the basis of general theoretical arguments and contain only very few free parameters. In this way satisfactory descriptions of several types of processes have been obtained [27, 28, 29, 30, 31, 32]. The data thus seem to confirm some general expectations concerning the dipole cross section, in and above the saturation region. Here we want to investigate whether the phenomenological models are compatible with the BK equation. We will compare the numerical solutions of the BK equation [22] with a recent model for the dipole cross section [29] that is intended to describe the momentum and x -dependence in a particular region above the saturation scale –the extended geometric scaling region. Our conclusions will also apply to the dipole models of [27, 32] in that region. Regarding the x -dependence it should be mentioned that the leading order BK equation is known [33, 34] to lead to a faster evolution in x ($Q_s^2(x) \sim 1/x^\lambda$ where $\lambda \simeq 0.9$ ¹) than the experimental data seem to favor ($\lambda \simeq 0.3$). This discrepancy can be reduced by introducing a running coupling constant and indeed in that case the DIS data seems to be describable taking both LO BK evolution and, for larger Q^2 , DGLAP evolution into account [35]. However, the consistency of including running coupling in an equation that is of leading order in α_s is questionable. This indicates that going beyond the leading order BK equation may be required in order to arrive at a proper quantitative comparison. Here however, we will be mainly interested in the question of whether the qualitative features of the models are reflected by the solutions to the leading order BK equation, especially around the saturation scale and at subasymptotic rapidities.

The outline of this paper is as follows. In Section II we discuss the properties of the phenomenological models of the dipole cross section in detail. In Section III the BK equation is briefly reviewed. Section IV is devoted to the study of the numerical solutions of the BK equation, by means of a comparison with a general Ansatz for the dipole cross section in terms of an anomalous dimension, in particular, the one proposed in Ref. [29]. We also study the x -dependence of the saturation scale with and without running coupling and consider the dependence of the results on the initial conditions. In Section V we summarize the main conclusions that can be drawn from the comparisons we have performed.

II. PHENOMENOLOGICAL STUDIES OF THE DIPOLE CROSS SECTION

A very successful phenomenological study of experimental data using a model for the dipole cross sections was performed by Golec-Biernat and Wüsthoff (GBW) [30]. The HERA data on the DIS structure function F_2 at low x ($x \lesssim 0.01$) they analyzed² could be described well by a dipole cross section of the form $\sigma = \sigma_0 N_{GBW}(r_t, x)$, where the scattering amplitude N_{GBW} is given by

$$N_{GBW}(r_t, x) = 1 - \exp \left[-\frac{1}{4} r_t^2 Q_s^2(x) \right], \quad (1)$$

r_t denotes the transverse size of the dipole, $\sigma_0 \simeq 23$ mb and the x -dependence of the saturation scale is given by

$$Q_s(x) = 1 \text{ GeV} \left(\frac{x_0}{x} \right)^{\lambda/2}, \quad (2)$$

with $x_0 \simeq 3 \times 10^{-4}$ and $\lambda \simeq 0.3$. Although here we discuss DIS off the proton ($A = 1$), we mention that for nuclear targets Q_s^2 increases as $A^{1/3}$.

¹ The exact value of λ depends on $\bar{\alpha}_s = N_c/\pi \alpha_s$, $\lambda \simeq 0.9$ corresponding to $\bar{\alpha}_s \simeq 0.2$.

² A further test of the dipole picture can be obtained from ratios of structure functions for which a bound has been derived recently [36].

The above scattering amplitude displays a characteristic feature called geometric scaling. This means that it depends on x and r_t^2 (r_t being the Fourier conjugate of $k_t = Q$) through the combination $r_t^2 Q_s^2(x)$ only. A model independent analysis of the DIS data from HERA shows that the low- x data display geometric scaling for all Q^2 [37], even though the GBW model, (1)-(2), was found to be inconsistent with newer, more accurate data [31] at large Q^2 . In Ref. [31] a modification of the GBW model was proposed which includes DGLAP evolution, as required to fit the $Q^2 > 20 \text{ GeV}^2$ data. Alternatively, in Ref. [35] the dipole scattering amplitude from the GBW model was replaced by a numerical solution to the leading order BK equation with running coupling and with the addition of a correction that satisfies DGLAP evolution in order to also describe the short distance behavior of N correctly. As emphasized in Ref. [32] (IIM), the solution to the BK equation (with running coupling) by itself only provides a satisfactory fit for relatively low Q^2 , up to a few GeV^2 .

As mentioned, the DIS data show geometric scaling for $x < 0.01$ and all Q^2 (this was recently confirmed in Ref. [38]), but the data above and below $Q^2/Q_s^2(x) \approx 1$ behave differently as a function of $Q^2/Q_s^2(x)$ [37]. On the basis of theoretical considerations one expects different geometric scaling behavior at low and high Q^2/Q_s^2 (a Gaussian-like function of Q^2/Q_s^2 at low Q^2/Q_s^2 and a power law fall-off at high Q^2/Q_s^2). Moreover, one expects an intermediate region, commonly referred to as the extended geometric scaling (EGS) region [34, 39, 40], starting from Q_s , extending to a scale Q_{gs} , where the geometric scaling behavior of the saturation region holds approximately. This EGS region grows with decreasing x .

An estimate of Q_{gs} has been obtained from the solution of the LO-BFKL evolution equation expanded to second order around the saturation saddle point [40]. Here Q_{gs} is taken to be the scale at which the violation of the geometric scaling behavior that holds at Q_s becomes of the same order as the leading order scaling contribution. One then finds $Q_{gs}(x) \sim Q_s^2(x)/\Lambda$, where Λ is a nonperturbative scale of order Λ_{QCD} . A similar result for Q_{gs} can be obtained from estimating the transition point between the LLA and DLA saddle points [41]. We emphasize that at Q_{gs} one does not necessarily observe large deviations from geometric scaling, one may also reach a region with a different geometric scaling behavior.

The theoretical studies of the EGS region have led IIM [32] to propose a modification to the GBW model so as to obtain a satisfactory fit to DIS data in both the saturation region and the EGS region, without including DGLAP evolution at large Q^2 . In the same spirit, KKT [27] have considered a modification of the GBW model in the EGS region in order to obtain a good description of the p_t spectra of hadron production at RHIC in $d\text{-Au}$ collisions (for a review of saturation physics and $d\text{-Au}$ collisions cf. [41]). Here we will restrict the discussion to the later modifications of the KKT model made by DHJ [29], but our conclusions for the EGS region will apply to the IIM and KKT models as well. We note that the saturation scale of the IIM model is to be multiplied by two in order to compare with the results obtained below. Other dipole models are discussed in Refs. [42, 43].

The model proposed by DHJ offers a good description of the p_t spectra of hadron production at RHIC in $d\text{-Au}$ collisions in both the midrapidity and forward regions, and even, as has been shown recently [44], the $p\text{-p}$ data in the very forward rapidity region.

The modified dipole scattering amplitude in the EGS region is given by [27, 28, 29]:

$$N(r_t, x) = 1 - \exp \left[-\frac{1}{4} (r_t^2 Q_s^2(x))^{\gamma(r_t, x)} \right]. \quad (3)$$

The exponent γ is usually referred to as the “anomalous dimension”, although the connection of N with the gluon distribution may not be clear for all cases considered below. This anomalous dimension γ changes the evolution in x , thus governing the possible violation of geometric scaling for scales between Q_s and Q_{gs} . The unitarized form of N is important only for scales around and below Q_s . For larger scales one can use to good approximation

$$N(r_t, x) \approx \frac{1}{4} (r_t^2 Q_s^2(x))^{\gamma(r_t, x)}, \quad (4)$$

which allows one to make a connection with the DGLAP region³, where $\tilde{N}_{\text{DGLAP}}(k_t, x) \propto k_t^{-4}$ (\tilde{N} being the Fourier transform defined in Eq. (7)), which is the tail behavior determined by one gluon (t -channel) exchange. Hence, the “DGLAP” limit of γ would be $\gamma \rightarrow 1$.

DHJ (following in part IIM and KKT) impose the following requirements to determine a parameterization of γ in the EGS region:

³ More specifically, at low x and high Q^2 a logarithmic evolution in both these variables may be required.

1. For any fixed x , in the limit $r_t \rightarrow 0$ γ should approach 1.
2. At the saturation scale, γ should be constant, so that N displays exact geometric scaling: $\gamma(r_t = 1/Q_s, x) = \gamma_s$. The constant γ_s is chosen to be $\simeq 0.628$.
3. If one writes $\gamma = \gamma_s + \Delta\gamma$, then $\Delta\gamma$ should decrease as $1/y$ for $y \rightarrow \infty$ at fixed $r_t^2 Q_s^2$.
4. At large, but fixed, rapidity y , the extent of the geometric scaling window should be consistent with the estimated scale $Q_{gs} = Q_s^2/\Lambda_{\text{QCD}}$.

A few comments on these requirements are in order. Requirement 1 is imposed in order to reproduce the ‘‘DGLAP’’ limit $N \sim r_t^2$. Requirement 2 and 3 were motivated by properties of the BFKL equation [32]. The idea is that since in the saddle point approximation the solution of the BFKL equation exhibits the property of geometric scaling, one can use it as an approximation to the solution of the BK equation near the saturation scale Q_s , provided that one imposes an appropriate boundary condition at Q_s [33, 34, 40], commonly referred to as a saturation boundary condition. Requirement 4 [29] is of a more phenomenological nature, and determines the speed with which γ increases from $\gamma_s \simeq 0.628$ at Q_s to a value near 1 at $Q_{gs} \approx Q_s^2/\Lambda_{\text{QCD}}$ (which is a function of y through Q_s). As can be seen from e.g. Ref. [41], requirement 3 is a prerequisite for requirement 4.

Following the above requirements, the anomalous dimension $\gamma(r_t, x)$ of DHJ is parameterized as [29]

$$\gamma(r_t, x) = \gamma_s + (1 - \gamma_s) \frac{\log(1/r_t^2 Q_s^2(x))}{\lambda y + d\sqrt{y} + \log(1/r_t^2 Q_s^2(x))}, \quad (5)$$

where $y = \log x_0/x$ is minus the rapidity of the target parton. The saturation scale $Q_s(x)$ and the parameter λ are taken from the GBW model, as given in Eq. (2). Requirement 4 is satisfied, which can be seen as follows: for large, but fixed rapidity ($y \gg (d/\lambda)^2$), the EGS region roughly extends to $\log Q_{gs}^2/Q_s^2 \sim \lambda y$, which implies that numerically $Q_{gs} \approx Q_s^2/\Lambda_{\text{QCD}}$. The parameterization (5) includes subleading corrections $\sim d\sqrt{y}$ which govern geometric scaling violations at subasymptotic rapidities. For $d \simeq 1.2$ a good description of d -Au data from RHIC over a considerable rapidity range, from mid- to forward rapidities, was obtained [29]. This parameter will play no role in our discussion, as we do not aim to obtain the best possible expression for either N or γ , but rather we want to investigate whether the above type of parameterization is compatible with the BK equation.

Two further aspects of DHJ’s Ansatz (3) for N with the anomalous dimension of Eq. (5) should be mentioned. First, in order to calculate observables (and to connect to the BK equation), one needs to formulate the dipole scattering amplitude in momentum space by performing a Fourier transform. To simplify this procedure, DHJ (following a similar step by KKT) replaced $\gamma(r_t, x)$ by $\gamma(1/k_t, x)$. This replacement should be viewed as an approximation that becomes better as k increases or equivalently, as r decreases. This simplifying approximation could be regarded as part of the Ansatz. Second, quarks and gluons are described by different scattering amplitudes, since they couple differently to the gluons. The above Ansatz (3) was applied by DHJ to gluons and is referred to as N_A . The corresponding expression for quarks is called N_F and is obtained from N_A by the replacement $Q_s^2 \rightarrow (C_F/C_A)Q_s^2 = (4/9)Q_s^2$. In the comparison to the GBW model, which is a model for N_F , one should take into account this factor, leading to $Q_s(x_0) = 1$ GeV instead of 0.67 GeV.

Eq. (5) was intended to parameterize γ in the geometric scaling window only, so the question arises what forms N takes in the saturation region, where $r_t > 1/Q_s$. For instance, it has been suggested [44] to be of the form (3) with γ a constant, equal to γ_s , so that the Ansatz for N displays exact geometric scaling throughout the saturation region. However, this idea has the drawback that the resulting N is not a smooth function of r_t , a problem also present in the IIM model. Its Fourier transform would therefore show artificial oscillations. To resolve this issue, it seems better to use the BK equation (or other, more appropriate, evolution equations) to determine the behavior of N in the saturation region. The goal of this paper is to study in more detail the relation between the DHJ Ansatz and the BK equation. We use the ‘‘BKsolver’’ program [45] to obtain a numerical solution to the BK equation and study whether the dipole profile of DHJ and similar models is consistent with this solution. Also, we will address the behavior of N in the saturation region as dictated by the BK equation. More specifically, we will investigate whether the requirements 2 and 3 on γ , which were motivated by the BFKL equation with a saturation boundary condition, are consistent with the nonlinear evolution of the BK equation.

III. BALITSKY-KOVCHegov EQUATION

The BK equation for N (more specifically, for N_F) reads [6, 7]

$$\frac{\partial N((\vec{x}_t - \vec{y}_t)^2, x)}{\partial y} = \frac{\bar{\alpha}_s}{2\pi} \int d^2 z_t \frac{(\vec{x}_t - \vec{y}_t)^2}{(\vec{x}_t - \vec{z}_t)^2 (\vec{y}_t - \vec{z}_t)^2} \left[N((\vec{x}_t - \vec{z}_t)^2, x) + N((\vec{z}_t - \vec{y}_t)^2, x) \right. \\ \left. - N((\vec{x}_t - \vec{y}_t)^2, x) - N((\vec{x}_t - \vec{z}_t)^2, x) N((\vec{z}_t - \vec{y}_t)^2, x) \right]. \quad (6)$$

Here $\bar{\alpha}_s = \alpha_s N_c / \pi$. We will not consider the impact parameter dependence of N in this paper.

Two types of Fourier transform are often considered in this context:

$$\tilde{N}(k, x) \equiv \int \frac{d^2 r_t}{2\pi} e^{i\vec{k}_t \cdot \vec{r}_t} N(r, x), \quad (7)$$

$$\mathcal{N}(k, x) \equiv \int \frac{d^2 r_t}{2\pi} e^{i\vec{k}_t \cdot \vec{r}_t} \frac{N(r, x)}{r^2}, \quad (8)$$

where $r^2 = \vec{r}_t^2$ and $k^2 = \vec{k}_t^2$. The first (regular) Fourier transform is the one that enters the cross section descriptions, such as the one considered by DHJ [28, 29]. The second transform, which includes the additional factor $1/r^2$, is more directly related to the (unintegrated) gluon distribution, as explained in detail in Ref. [51]. In terms of \mathcal{N} , the BK equation can be very compactly written as

$$\partial_Y \mathcal{N} = \chi(-\partial_L) \mathcal{N} - \mathcal{N}^2, \quad (9)$$

where $Y = y \bar{\alpha}_s$, $L = \log(k^2/k_0^2)$, for some arbitrary scale k_0 , and $\chi(\gamma)$ is the BFKL kernel,

$$\chi(\gamma) = 2\psi(1) - \psi(\gamma) - \psi(1 - \gamma). \quad (10)$$

In the limit of large k ($\gg Q_s$), or equivalently, small r , the nonlinear BK equation (9) reduces to the linear BFKL equation. In the saddle point approximation, the solution of the BFKL equation behaves as $N(r, x) \sim r^{2\gamma'}$ for small r , hence the exponent γ' determines the small- r limit of the anomalous dimension γ through Eq. (4). Therefore, γ is determined by either the BFKL saddle point $\gamma_{s.p.}$ or the initial condition: if in the limit $r \rightarrow 0$ the starting distribution has the property $N(r, x_0) \sim r^{2\gamma_0}$, then for any fixed x the asymptotically small r behavior either remains $r^{2\gamma_0}$ if $\gamma_0 < \gamma_{s.p.}$, or becomes $r^{2\gamma_{s.p.}}$ if $\gamma_0 \geq \gamma_{s.p.}$. We will demonstrate this observation explicitly below. For finite x , the BFKL saddle point approaches $\gamma_{s.p.} \approx 1$ in the limit of small r , cf. e.g. [40]. Therefore, any solution to the BK equation will only satisfy requirement 1 of DHJ if the starting distribution in the small- r limit has the property that $\gamma_0 \geq 1$.

Around the saturation scale, the solution of the BK equation has been approximated by a solution of the BFKL equation which has been required to satisfy a saturation boundary condition [33, 34, 40]. This leads to the aforementioned saddle point at saturation, $\gamma_s \approx 0.628$, which is the solution of the equation $\chi(\gamma_s)/\gamma_s = \chi'(\gamma_s)$ [4, 40]. However, unlike in the small- r limit where the BFKL solution and Eq. (3) reduce to the same form, around the saturation scale there is no clear correspondence between this saddle point and the anomalous dimension of Eq. (3).

Alternatively, one can first approximate the BK equation (9) by expanding the kernel χ around the saddle point, and subsequently solve the resulting equation analytically. This has been done in Refs. [9, 10, 11, 12] where a traveling wave solution has been obtained that is valid in a finite range of k , which grows with the rapidity. The value $\gamma_s \approx 0.628$ enters the analytic expressions for $\mathcal{N}(k, x)$ of the traveling wave solutions⁴. However, also for this solution γ_s does not correspond directly to the anomalous dimension of Eq. (3) at the saturation scale, since there is no direct relation between $N(r, x)$ and $\mathcal{N}(k, x)$ at the respective points $r = 1/Q_s$ and $k = Q_s$.

We conclude that requirement 2 of DHJ, which sets γ at the saturation scale equal to $\gamma_s \approx 0.628$, does not follow from these analytical results. For completeness we mention that other analytical aspects of the solutions of the BK equation, such as the small- k limit, have been investigated as well [8, 13, 14].

⁴ For initial conditions with $\gamma_0 < \gamma_s$, γ_s is replaced with γ_0 in the traveling wave expression.

Here, we will restrict ourselves to comparing the phenomenological DHJ model with numerical solutions. Such solutions have been obtained by several groups [15, 16, 17, 18, 19, 20, 21, 22], even including impact parameter dependence [47, 48, 49, 50]. The code employed by the authors of Ref. [22] to numerically solve the BK equation has been made publicly available [45]. We will use this code in our subsequent investigation of the DHJ Ansatz and its possible extension to the saturation region. But first we want to point out that these numerical solutions do not show geometric scaling for finite rapidities. The deviations can become significant even in the saturation region at moderate y . As is known, in the limit of large rapidities, geometric scaling is recovered; $\mathcal{N}(k, x)$ is given by a function \mathcal{N}_∞ that depends on $k/Q_s(x)$ only. Fig. 1a shows the relative difference between \mathcal{N} and the asymptotic solution \mathcal{N}_∞ as a function of $k/Q_s(x)$. The saturation scale $Q_s(x)$ is defined as the value of k where \mathcal{N} equals some arbitrary fixed value for which \mathcal{N}^2 becomes non-negligible. Based on our study in Sec. IV.B we have chosen $\mathcal{N}(Q_s(x), x) = 0.2$. Due to this definition $\mathcal{N} - \mathcal{N}_\infty$ vanishes at the saturation scale. Clearly, the scaling violations in the saturation region are considerable for finite rapidities. Fig. 1b shows the dipole scattering amplitude $N(r, x)$ in coordinate space as it follows by a Fourier transformation (11) from $\mathcal{N}(k, x)$. As expected, $N(r, x)$ vanishes for small r and approaches 1 in the saturation region $r \gg 1/Q_s(x)$. Like in momentum space $N(r, x)$ approaches a limiting curve that depends only on $rQ_s(x)$ and geometric scaling is recovered. Throughout this paper we have chosen a constant coupling $\bar{\alpha}_s = N_c/\pi \alpha_s \approx 0.2$.

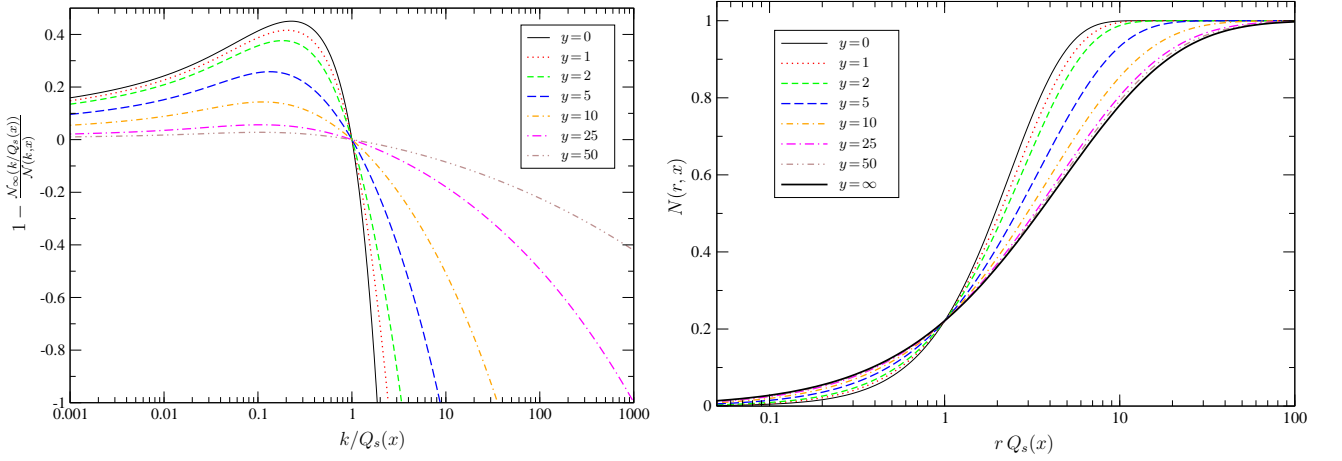


FIG. 1: a) The relative difference $1 - \mathcal{N}_\infty(k/Q_s(x))/\mathcal{N}(k/Q_s(x), x)$ between the function $\mathcal{N}(k, x)$ (8) following from the BK equation and its geometrically scaling asymptotic $\lim_{x \rightarrow 0} \mathcal{N}(k/Q_s(x), x) = \mathcal{N}_\infty(k/Q_s(x))$ for various rapidities $y = \log x_0/x$. b) The dipole scattering amplitude $N(r, x)$ resulting from a Fourier transformation (11) of $\mathcal{N}(k, x)$ as a function of $rQ_s(x)$ for various rapidities $y = \log x_0/x$.

IV. ANOMALOUS DIMENSION FROM THE BALITSKY-KOVCHegov EQUATION

A. Anomalous dimension as a function of r and x

The BKSolver program [45] provides numerical values for the amplitude $\mathcal{N}(k, x)$ as a function in momentum space. In order to use this solution of the BK equation to constrain $\gamma(r, x)$, one first has to find $N(r, x)$ by Fourier transforming back to coordinate space:

$$N(r, x) = r^2 \int \frac{d^2 k_t}{2\pi} e^{-i\vec{k}_t \cdot \vec{r}_t} \mathcal{N}(k, x) = r^2 \int_0^\infty dk k J_0(kr) \mathcal{N}(k, x). \quad (11)$$

Using the Ansatz (3) one can extract $\gamma(r, x)$ from the resulting $N(r, x)$,

$$\gamma(r, x) = \frac{\log \left[\log \left[\frac{1}{(1-N(r, x))^4} \right] \right]}{\log[r^2 Q_s^2(x)]}. \quad (12)$$

This equation requires as a separate input the value of $Q_s(x)$, which can be found as follows. One can fix $Q_s(x)$ in such a way that at the saturation scale the amplitude obtained from the BK equation (12) equals the Ansatz (3), which at Q_s becomes independent of γ ,

$$N(r = 1/Q_s, x) = 1 - \exp[-1/4] \approx 0.22. \quad (13)$$

Equating this fixed value with the general relation (11) allows one to calculate the saturation scale $Q_s(x)$ by solving the following equation,

$$\frac{1}{Q_s^2(x)} \int_0^\infty dk k J_0(k/Q_s(x)) N(k, x) = 1 - \exp[-1/4]. \quad (14)$$

Combining the resulting values of the saturation scale with Eq. (12), we obtain a numerical result for $\gamma(r, x)$, which is shown in Fig. 2 as a function of $1/(rQ_s(x))$. This means that the saturation region is located to the left of 1 on the horizontal axis, so that it is easier to compare with later figures that display related quantities as a function of k/Q_s . Note that although the Ansatz (3) was specifically intended to describe N in the EGS region, we also show γ in the saturation region.

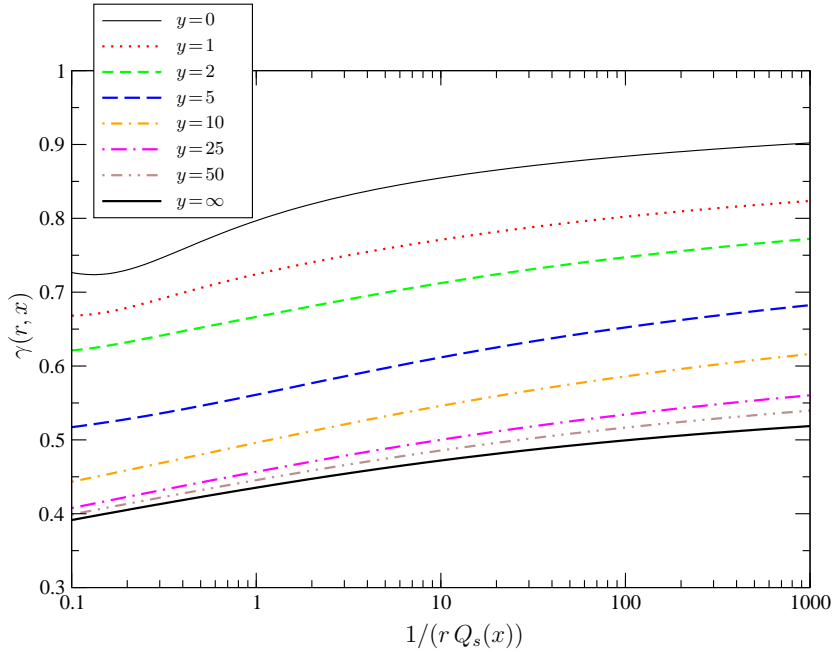


FIG. 2: $\gamma(r, x)$ resulting from the relations (11) and (12) as a function of $1/(rQ_s(x))$ and $y = \log x_0/x$.

The resulting $\gamma(r, x)$ has the following features:

1. For $r \rightarrow 0$, $\gamma(r, x)$ asymptotically approaches 1.
2. At the saturation scale, $\gamma(r, x)$ is not a constant.
3. For decreasing x , $\gamma(r, x)$ approaches a limiting curve, indicated in Fig. 2 by $y = \infty$. Hence, after a longer evolution one indeed recovers geometric scaling.

The fact that for small distances γ asymptotically approaches 1 is understandable from the BK equation, since in this limit it reduces to the BFKL equation. As mentioned before, in the limit of small distances, the solution to the BFKL equation is dominated by either the saddle point or the initial condition, both leading to $\gamma \rightarrow 1$, since here we use the MV model (17) as the initial condition.

Requirement 2 of the DHJ Ansatz is clearly not satisfied by the numerical solution of the BK equation at the saturation scale. Instead of writing $\gamma(r, x) = \gamma_s + \Delta\gamma(r, x)$, it seems more natural to consider the following

split-up:

$$\gamma(r, x) = \gamma_\infty(rQ_s(x)) + \Delta\gamma(r, x), \quad (15)$$

where it turns out that, similar to requirement 3, $\Delta\gamma(r, x)$ decreases as $1/y$ for $y \rightarrow \infty$ and fixed $rQ_s(x)$. At the saturation scale γ is given in the small- x limit by,

$$\lim_{x \rightarrow 0} \gamma(r = 1/Q_s(x), x) = \gamma_\infty(1) \approx 0.44, \quad (16)$$

a value that is significantly below $\gamma_s = 0.628$.

It would be interesting to see whether the numerically obtained γ could fit the available data as well, which does not seem unlikely since KKT employed $\gamma_s = 0.5$ and were able to fit d -Au data, but this is not the aim of the present paper, where we instead focus on the comparison of existing models for the dipole cross section with the numerical solution of the BK equation. Moreover, a word of caution has to be added about the results for small values of y (below $y = 5$, say): the numerical solutions are obtained after a choice of a starting distribution at $y = 0$ ($x = x_0$). For “short” evolutions (small y -values), the properties of the starting distribution are still visible in the result, i.e. not only in the small- r limit. The starting distribution should be appropriate to the choice of x_0 , which itself should be small enough for BK evolution to be applicable. If x_0 is sufficiently small, or alternatively if A is sufficiently large, one can take for instance the McLerran-Venugopalan (MV) model [24]. One could also consider taking the DHJ model, which however is restricted to the EGS region, therefore requiring some extrapolation to the entire r or k range. For larger values of x_0 one may consider using one of the standard parton distributions, although these are not defined over the whole range either.

Due to this problem, throughout this paper we have used the MV model as a starting distribution⁵:

$$N(r, x) = 1 - \exp \left[-\frac{1}{4} (r^2 Q_s^2(x)) \log(e + 1/(r^2 \Lambda^2)) \right], \quad (17)$$

which is one of the distributions considered in Ref. [22]. In Sec IV.E we show some results for another choice of starting distribution, to illustrate the influence of the initial condition. The dependence of the numerical results on the starting distribution has also been investigated in Ref. [22], to which we refer for additional information.

Hence, for small rapidities ($y \lesssim 5$) one should avoid drawing too strong conclusions from a comparison of the DHJ parameterization with the numerical results that were obtained with the MV starting distribution. Nevertheless, we will be able to draw some qualitative conclusions also for lower y -values from our results in Sec IV.B.

B. The replacement $\gamma(r, x) \rightarrow \gamma(1/k, x)$

As mentioned before, DHJ actually considered Eq. (3) with $\gamma(r, x)$ replaced by $\gamma(1/k, x)$ [27, 28, 29]. This approximation scheme we will discuss next. The procedure of extracting γ becomes quite different when γ depends on k , since the dipole cross section N then depends on both r and k , so that it is not related to $\mathcal{N}(k, x)$ by a straightforward inverse Fourier transform (11) anymore:

$$\mathcal{N}(k, x) \equiv \int_0^\infty \frac{dr}{r} J_0(kr) \left(1 - \exp \left[-\frac{1}{4} (r^2 Q_s^2(x))^{\gamma(k, x)} \right] \right). \quad (18)$$

Instead of by the inverse Fourier transform, we will extract γ by trying to numerically solve Eq. (18), imposing the following condition. In order to test the Ansatz of DHJ, we will fix $\gamma(k, x)$ in such a way that it equals the constant γ_s at the saturation scale:

$$\gamma(Q_s(x), x) = \gamma_s \approx 0.628. \quad (19)$$

⁵ There are many ways in which the infrared divergence that occurs in the MV model can be regularized; the replacement of $\log(1/(r^2 \Lambda^2)) \rightarrow \log(e + 1/(r^2 \Lambda^2))$ is one option. In Ref. [52] it is shown that the results do not depend much on the choice of regularization.

This determines the dependence of Q_s on x , which can be found by explicitly solving

$$\mathcal{N}(Q_s(x), x) = \int_0^\infty \frac{dz}{z} J_0(z) \left(1 - \exp \left[-\frac{1}{4}(z^2)^{\gamma_s} \right] \right) \approx 0.19. \quad (20)$$

Now we can extract γ from relation (18) for any given value of x and k . Fig 3 shows the results for $\gamma(k, x)$ as a function of k/Q_s in the EGS region, for a broad range of rapidities. For small rapidities the resulting γ looks very similar to the one of DHJ (cf. Fig. 4 of Ref. [29]). This gives us an indication of how the DHJ distribution would behave under BK evolution. We reiterate that one cannot use the DHJ distribution itself as a starting distribution as it is not defined over the whole r or k range. As one can see, for larger y the resulting γ is not compatible with the DHJ parameterization (5) anymore; it first decreases ($\Delta\gamma < 0$) before it rises towards 1 asymptotically.

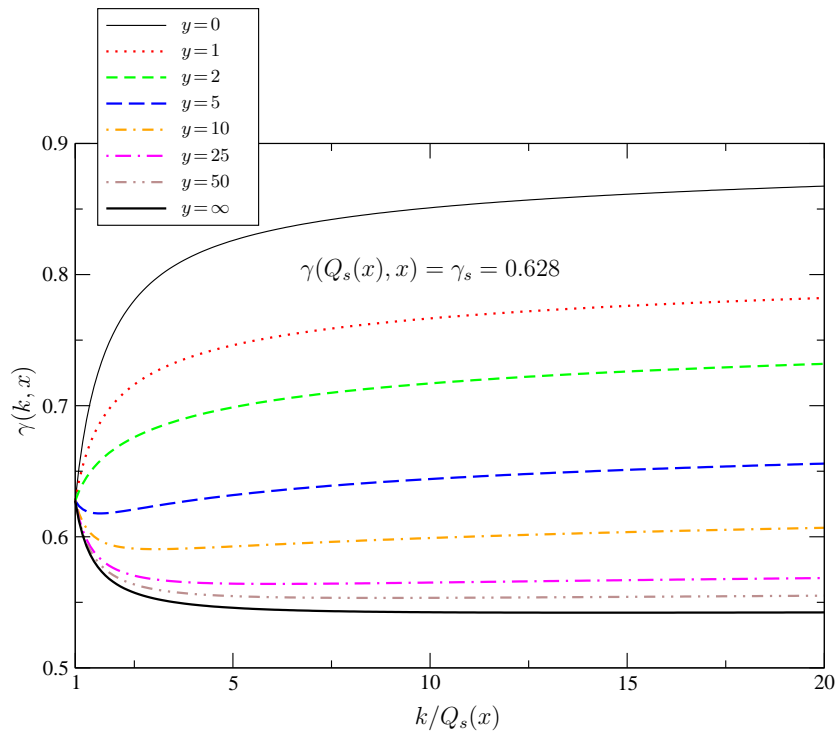


FIG. 3: $\gamma(k, x)$ as a function of $k/Q_s(x)$ for various rapidities $y = \log x_0/x$.

In Fig. 4 the same result is shown but now for a smaller choice of constant γ at the saturation scale, $\gamma(k = Q_s, x) = 0.44$. This value is the small- x limit (16) of $\gamma(r = 1/Q_s(x), x)$ in the approach of the previous subsection. In this case $\Delta\gamma$ remains positive above the saturation scale and the result looks very much like the DHJ parameterization for all y . A fit of γ as given in Eq. (5) to the numerical results for $k/Q_s = 1, 2, \dots, 5$ and rapidities $y = 1, 2, \dots, 5$ (in order to allow for a comparison to DHJ's results) yields $\lambda \approx 1$ and $d \approx 3$, although it must be emphasized that the shapes of the curves are not exactly of the form (5).

C. The saturation region

The DHJ Ansatz was specifically intended to describe the dipole scattering amplitude in the EGS region, but it is nevertheless interesting to see what γ will look like if one were to assume the same form of N in the saturation region. One may expect the solution to be geometrically scaling in the region $r \geq 1/Q_s$, which would be the case if $\gamma(r, x) = \gamma(rQ_s(x))$. A constant γ would of course be a special case. However, the numerical solution of the BK equation does not display geometric scaling, not even in the saturation region, although for large rapidities $\mathcal{N}(k, x)$, as a function of $k/Q_s(x)$, converges to a well-defined limit. The same conclusion applies to γ upon assuming the Ansatz (3) for $N(r, x)$. This is clearly seen in Fig. 2.

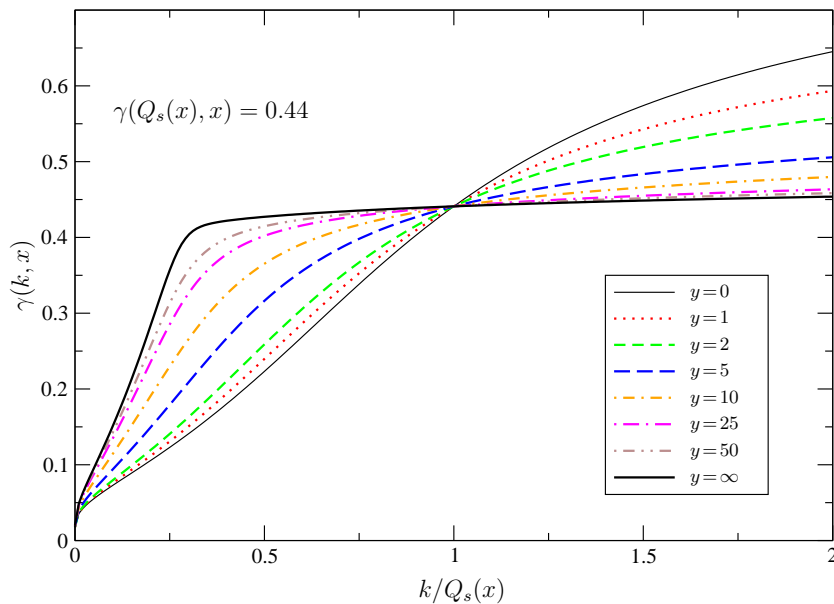


FIG. 4: $\gamma(k, x)$ as a function of $k/Q_s(x)$ for various rapidities $y = \log x_0/x$.

The situation is similar if we replace $\gamma(r, x)$ with $\gamma(1/k, x)$, keeping γ at the saturation scale $k = Q_s$ fixed, with the exception that in some cases no solutions for γ can be found at all in the saturation region. The existence of a solution in a certain range of k/Q_s depends on the chosen saturation scale or, in the above discussed approach, equivalently, on the fixed value of γ at the saturation scale, which determines the saturation scale. In fact, we find that if $\gamma(k = Q_s(x), x)$ is fixed to equal $\gamma_s = 0.628$, the Ansatz (3) is not compatible with the solution of the BK equation in the range $k/Q_s \approx 0.2 - 0.4$, where no value of $\gamma(k, x)$ satisfies the relation (18) for large rapidities. If instead we fix γ at the saturation scale to equal the limit (16), the saturation scale is shifted towards smaller values, so that there is a unique solution for γ for all k and x . Above the saturation scale $\gamma(k, x)$ is in agreement with the type of parameterization of DHJ (5). For asymptotic rapidities, γ approaches a limiting curve, which is geometrically scaling for all k values, not just at the saturation scale (which was the case by construction). Note that below the saturation scale the solution is far from constant, although for large rapidities the solution is rather constant for a considerable momentum range below Q_s . But eventually, for very small k , it drops significantly to a small nonvanishing value. We emphasize that this is the case under the assumption that the form (3) also holds for momenta below the saturation scale. Let us mention that in the region where γ eventually drops towards smaller values $r Q_s(x)$ becomes effectively already so large that $N(r, x) \approx 1$, so that the exact value of γ eventually becomes irrelevant, see Fig. 1b.

D. Saturation scale dependence on x

In Fig. 5 we display the values of $Q_s(x)$ for a fixed coupling $\bar{\alpha}_s = 0.2$ as a function of $y = \log x_0/x$, in order to show that (at least for larger rapidities, $y > 10$ say) the behavior $Q_s(x) \sim x^{-\lambda/2}$ is found in all scenarios considered here. The values of the parameters can be compared with the GBW values of $\lambda \simeq 0.3$ and $Q_s(y = 0) \simeq 1$ GeV. We note that strictly speaking one has to include a factor $2/3$ in $Q_s(y = 0)$ if the DHJ Ansatz for N_F is used for calculating $Q_s(x)$. This is the case in e.g. Eqs. (14) and (20). The larger value of $\lambda \approx 0.9$ is in agreement with the asymptotic result $\lambda \approx \bar{\alpha}_s \chi(\gamma_s)/\gamma_s \approx \bar{\alpha}_s 4.88$ from LO BFKL equation with saturation boundary conditions [34] and $\lambda = 4\bar{\alpha}_s$ from the DLA approach [13, 21, 39, 40].

We have also investigated the case where the coupling constant runs with the energy scale, which is given by the inverse of the relevant dipole size. For details, we refer to [22, 45]. The energy scale turns out to be effectively of the order of the resulting saturation scale Q_s . The running of the coupling results in a change in the dependence of $Q_s(x)$ on x , for which we now find approximately $Q_s(y) = Q_s(0) \exp[c\sqrt{y}/2]$, which in fact is equally well supported by all relevant DIS data [38]. Since we have plotted every result for the anomalous dimensions as

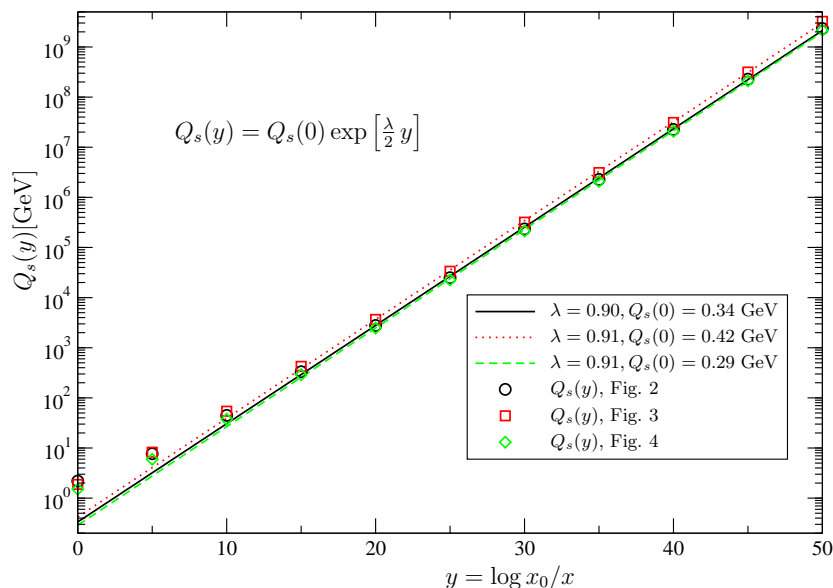


FIG. 5: The saturation scale from the various approaches for $y = \log x_0/x = 0, 5, 10, \dots, 50$ (symbols) and the related fits of the form $Q_s(y) = Q_s(0) \exp[\lambda y/2]$ in the fixed coupling case, where $\bar{\alpha}_s = 0.2$.

a function of dimensionless quantities, i.e. $rQ_s(x)$ or $k/Q_s(x)$, none of those results is significantly affected by including running in the coupling constant. It has to be mentioned that since the BK equation is of leading order in α_s , including the running coupling is of course not a consistent treatment of higher order effects. For that reason we mainly focus on the fixed coupling case.

E. Dependence on the initial conditions

To illustrate the dependence of some of our results on the choice of a starting distribution, we replace the MV distribution with the following choice:

$$N(r, x = x_0) = 1 - \exp \left[-\frac{1}{4} (r^2 Q_s^2(x = x_0))^{\gamma_0} \right]. \quad (21)$$

Fig. 6a shows the resulting $\gamma(r, x)$ as a function of $1/(rQ_s(x))$ for the initial conditions $\gamma_0 = 0.6, 1$ and 1.1 , in a very large r range in order to display the asymptotic small- r behavior. As expected from the discussion in Sec. III, in the limit of very large $1/(rQ_s)$ at finite rapidity, γ approaches either the initial condition γ_0 , if $\gamma_0 < 1$, or the saddle point, which is 1 in this limit.

Fig. 6b shows a similar plot for the initial conditions $\gamma_0 = 0.5, 0.6$ and 0.7 at larger rapidities. For $\gamma_0 = 0.5$ in the large- y limit γ approaches a limiting function that monotonically rises towards γ_0 at small rQ_s . The limiting function for $\gamma_0 = 0.6$ behaves similarly. For $\gamma_0 = 0.7$ the limiting function coincides to good approximation with the one of $\gamma_0 = 0.6$ up to small values of rQ_s , but becomes slightly larger as rQ_s decreases further. In the entire investigated range the limiting function of $\gamma_0 = 0.7$ coincides with the one of the MV starting distribution (17), partly shown in Fig. 2. We conclude that if $\gamma_0(rQ_s)$ is sufficiently large, one always reaches a universal limiting function $\gamma_\infty(rQ_s)$. This function equals approximately 0.44 at the saturation scale and approaches a limit $\gamma_\infty(rQ_s \rightarrow 0)$ which seems to be slightly larger than 0.6. As discussed below, the latter limit seems consistent with the theoretical expectation of 0.628. In the specific case of constant γ_0 the universal limiting curve is always reached if γ_0 is larger than $\gamma_\infty(rQ_s \rightarrow 0)$.

A similar dependence on γ_0 has been observed in Ref. [10] on the traveling wave solution. This solution depends on a parameter γ which equals either γ_s or γ_0 , whichever is the smallest. In our approach the role of γ_s of the traveling wave is played by the function γ_∞ . At large k/Q_s and y the traveling wave solution is dominated by the term $(k^2/Q_s^2(x))^{-\gamma}$, leading to the previously mentioned expectation that $\gamma_\infty(rQ_s \rightarrow 0) = \gamma_s$.

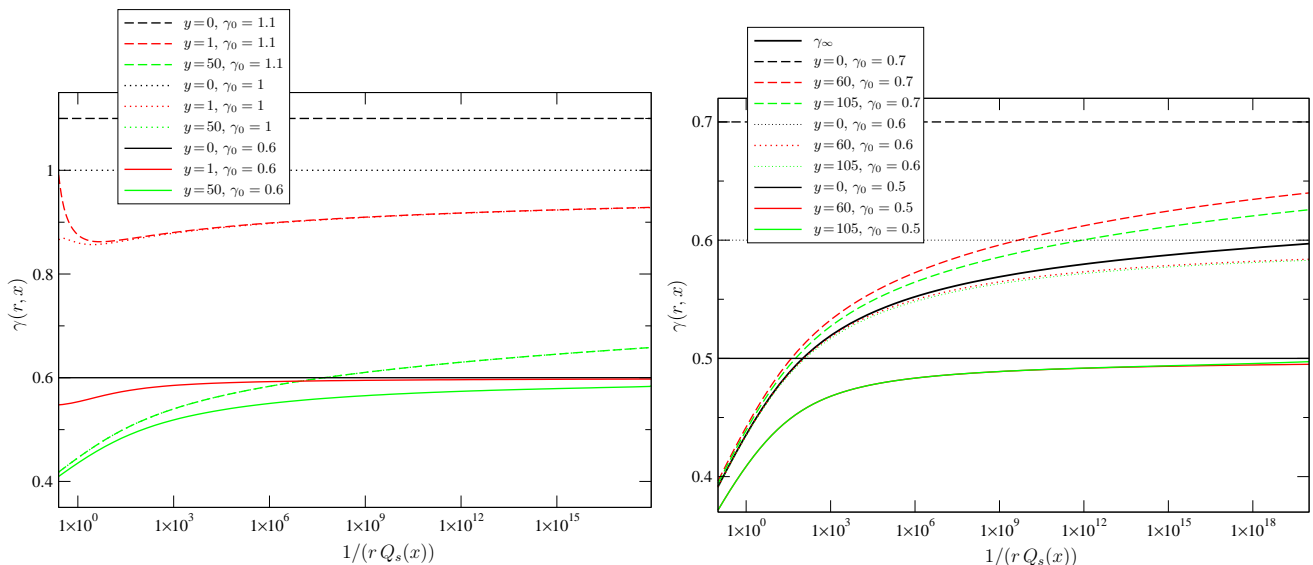


FIG. 6: a) $\gamma(r, x)$ for three different rapidities and initial conditions $\gamma_0 = 0.6, 1, 1.1$. To illustrate the small r asymptotics, we show $\gamma(r, x)$ over a very large range. Note that the curves with $\gamma_0 = 1$ and 1.1 for $y = 50$ are hard to distinguish. b) $\gamma(r, x)$ as a function of $1/(rQ_s(x))$ and initial conditions $\gamma_0 = 0.5, 0.6$ and 0.7 for large rapidities $y = \log x_0/x$. Here, the curves for $y = 60$ and $y = 105$ largely coincide for both $\gamma_0 = 0.5$ and 0.6 .

Finally, we compare our results to those of Ref. [49], especially Fig. 4. There it is found that for small rQ_s the scattering amplitude can be described by $N(r) = a(rQ_s)^{2\gamma}(\log(rQ_s) + \delta)$, where γ approaches approximately 0.65 for large y , regardless of the initial condition. We find that the particular value of 0.65 is consistent with our result for γ_∞ , if we take into account the different functional form for $N(r, x)$ and the specific range of r and y in which γ was calculated. However, even for $\gamma_0 = c/2 = 0.42$, Ref. [49] find no dependence of γ on the initial condition, which seems to disagree with our results and those of Ref. [10].

V. CONCLUSIONS

The numerical solutions of the BK equation do not display exact geometric scaling, although they approach a solution showing such scaling at asymptotic y . Assuming the solutions to be of the form (3), where scaling violations are encoded in the “anomalous dimension” γ , therefore leads to the conclusion that $\gamma(r, x)$ is not a function of $rQ_s(x)$ exclusively. In particular, it is never simply a constant, not even at the saturation scale ($r = 1/Q_s$). At asymptotically large rapidities, γ reaches a limiting function $\gamma_\infty(rQ_s(x))$. This function is universal for a large range of initial conditions. At the saturation scale, this function equals approximately 0.44, which is considerably smaller than the corresponding values of γ in the phenomenological models [27, 29, 32]. For small values of rQ_s the limiting function seems to reach γ_s , in accordance with the traveling wave results of Refs. [9, 10]. This is not in contradiction with the behavior of γ in the limit of $rQ_s(x) \rightarrow 0$ at any fixed x , where γ is determined by the starting distribution or the BFKL saddle point. It merely implies that the two limits $rQ_s(x) \rightarrow 0$ and $x \rightarrow 0$ do not commute.

Although the numerical solutions of the BK equation lead to a $\gamma(r, x)$ that is never a constant as a function of x at the saturation scale, performing the replacement of $\gamma(r, x) \rightarrow \gamma(1/k, x)$ does allow one to find a solution for which $\gamma(k = Q_s, x)$ is kept fixed. The behavior of $\gamma(1/k, x)$ is then qualitatively similar to the DHJ parameterization for small rapidities. However, the usually considered choice $\gamma(k = Q_s, x) = \gamma_s = 0.628$ yields some unwanted features, i.e. the fact that $\Delta\gamma < 0$ in a region above the saturation scale and the absence of solutions below the saturation scale, although the Ansatz was not intended for that region. Keeping $\gamma(k = Q_s, x)$ fixed at a smaller value, e.g. at $\gamma_\infty(rQ_s = 1) \approx 0.44$, seems more suitable, but it remains to be investigated whether such a choice allows for a good fit of all relevant DIS, d -Au and p -p data. One might expect this to be possible, as the KKT model [27], which has $\gamma = 0.5$ at the saturation scale, is able to describe the d -Au data.

The resulting saturation scales in the various approaches we adopted, evolve quite similarly with decreasing x , namely approximately as $Q_s(x) = Q_s(x_0)(x_0/x)^{\lambda/2}$, albeit with somewhat different normalizations $Q_s(x_0)$. In the case of a running coupling constant, the dependence on y changes from $\exp(\lambda y/2)$ to $\exp(c\sqrt{y}/2)$, which is equally well supported by all relevant DIS data [38].

Our conclusions about the DHJ model apply as well to the IIM and KKT models in the EGS region. It would be interesting to consider modifications of these models for the dipole scattering amplitude that are compatible with both the BK equation and the data. Given the fact that the BK evolution does not respect geometric scaling around Q_s , phenomenological parameterizations that reflect this feature would seem a natural choice. Fortunately, the LHC and a possible future electron-ion collider will provide data over a larger range of momenta and rapidities, so that one can expect to test the evolution properties of the models more accurately.

Acknowledgments

D.B. thanks Adrian Dumitru, François Gelis, Arata Hayashigaki, Dima Kharzeev, Kazunori Itakura, Larry McLerran, Kirill Tuchin and Raju Venugopalan, for sharing their knowledge on this topic with him on several occasions. We thank Adrian Dumitru for helpful comments on the manuscript. We thank one of the referees for helping to clarify the role of the initial condition and for pointing out the apparent discrepancy of our results with those of Ref. [49]. This research is part of the research program of the “Stichting voor Fundamenteel Onderzoek der Materie (FOM)”, which is financially supported by the “Nederlandse Organisatie voor Wetenschappelijk Onderzoek (NWO)”.

-
- [1] A. H. Mueller, Nucl. Phys. B **335**, 115 (1990).
 - [2] E. A. Kuraev, L. N. Lipatov and V. S. Fadin, Sov. Phys. JETP **45**, 199 (1977) [Zh. Eksp. Teor. Fiz. **72**, 377 (1977)].
 - [3] I. I. Balitsky and L. N. Lipatov, Sov. J. Nucl. Phys. **28**, 822 (1978) [Yad. Fiz. **28**, 1597 (1978)].
 - [4] L. V. Gribov, E. M. Levin and M. G. Ryskin, Phys. Rept. **100**, 1 (1983).
 - [5] E. Laenen and E. Levin, Nucl. Phys. B **451**, 207 (1995).
 - [6] I. Balitsky, Nucl. Phys. B **463**, 99 (1996).
 - [7] Y. V. Kovchegov, Phys. Rev. D **60**, 034008 (1999).
 - [8] Y. V. Kovchegov, Phys. Rev. D **61**, 074018 (2000).
 - [9] S. Munier and R. Peschanski, Phys. Rev. Lett. **91**, 232001 (2003).
 - [10] S. Munier and R. Peschanski, Phys. Rev. D **69**, 034008 (2004).
 - [11] C. Marquet, R. Peschanski and G. Soyez, Nucl. Phys. A **756**, 399 (2005).
 - [12] C. Marquet, R. Peschanski and G. Soyez, Phys. Lett. B **628**, 239 (2005).
 - [13] E. Levin and K. Tuchin, Nucl. Phys. B **573**, 833 (2000).
 - [14] M. Kozlov and E. Levin, Nucl. Phys. A **764**, 498 (2006).
 - [15] M. Braun, Eur. Phys. J. C **16**, 337 (2000).
 - [16] M. A. Braun, arXiv:hep-ph/0101070.
 - [17] M. Lublinsky, Eur. Phys. J. C **21**, 513 (2001).
 - [18] M. Lublinsky, E. Gotsman, E. Levin and U. Maor, Nucl. Phys. A **696**, 851 (2001).
 - [19] N. Armesto and M. A. Braun, Eur. Phys. J. C **20**, 517 (2001).
 - [20] E. Levin and M. Lublinsky, Nucl. Phys. A **696**, 833 (2001).
 - [21] K. Golec-Biernat, L. Motyka and A. M. Stasto, Phys. Rev. D **65**, 074037 (2002).
 - [22] R. Enberg, K. Golec-Biernat and S. Munier, Phys. Rev. D **72**, 074021 (2005).
 - [23] A. M. Stasto, Acta Phys. Polon. B **35**, 3069 (2004).
 - [24] L. McLerran and R. Venugopalan, Phys. Rev. D **49**, 2233 (1994); *ibid.* **49**, 3352 (1994); Y. V. Kovchegov, *ibid.* **54**, 5463 (1996); *ibid.* **55**, 5445 (1997).
 - [25] E. Iancu, A. Leonidov and L. McLerran, arXiv:hep-ph/0202270; E. Iancu and R. Venugopalan, arXiv:hep-ph/0303204.
 - [26] J. Jalilian-Marian, A. Kovner, A. Leonidov and H. Weigert, Nucl. Phys. B **504**, 415 (1997); Phys. Rev. D **59**, 014014 (1999); E. Iancu, A. Leonidov and L. D. McLerran, Nucl. Phys. A **692**, 583 (2001); Phys. Lett. B **510**, 133 (2001); E. Ferreira, E. Iancu, A. Leonidov and L. McLerran, Nucl. Phys. A **703**, 489 (2002); I. Balitsky, Phys. Lett. B **518**, 235 (2001).
 - [27] D. Kharzeev, Y. V. Kovchegov and K. Tuchin, Phys. Lett. B **599**, 23 (2004).
 - [28] A. Dumitru, A. Hayashigaki and J. Jalilian-Marian, Nucl. Phys. A **765**, 464 (2006).
 - [29] A. Dumitru, A. Hayashigaki and J. Jalilian-Marian, Nucl. Phys. A **770**, 57 (2006).

- [30] K. Golec-Biernat and M. Wüsthoff, Phys. Rev. D **59**, 014017 (1999).
- [31] J. Bartels, K. Golec-Biernat and H. Kowalski, Phys. Rev. D **66**, 014001 (2002).
- [32] E. Iancu, K. Itakura and S. Munier, Phys. Lett. B **590**, 199 (2004).
- [33] D. N. Triantafyllopoulos, Nucl. Phys. B **648**, 293 (2003).
- [34] A. H. Mueller and D. N. Triantafyllopoulos, Nucl. Phys. B **640**, 331 (2002).
- [35] E. Gotsman, E. Levin, M. Lublinsky and U. Maor, Eur. Phys. J. C **27**, 411 (2003).
- [36] C. Ewerz and O. Nachtmann, arXiv:hep-ph/0611076.
- [37] A. M. Stasto, K. Golec-Biernat and J. Kwiecinski, Phys. Rev. Lett. **86**, 596 (2001).
- [38] F. Gelis, R. Peschanski, G. Soyez and L. Schoeffel, arXiv:hep-ph/0610435.
- [39] E. Levin and K. Tuchin, Nucl. Phys. A **691**, 779 (2001).
- [40] E. Iancu, K. Itakura and L. McLerran, Nucl. Phys. A **708**, 327 (2002).
- [41] J. Jalilian-Marian and Y. V. Kovchegov, Prog. Part. Nucl. Phys. **56**, 104 (2006).
- [42] V. P. Goncalves, M. S. Kugeratski, M. V. T. Machado and F. S. Navarra, Phys. Lett. B **643**, 273 (2006).
- [43] J. T. de Santana Amaral, M. A. Betemps, M. B. Gay Ducati and G. Soyez, arXiv:hep-ph/0612091.
- [44] D. Boer, A. Dumitru and A. Hayashigaki, Phys. Rev. D **74**, 074018 (2006).
- [45] R. Enberg, “BKsolver: numerical solution of the Balitsky-Kovchegov nonlinear integro-differential equation”, available at URL: <http://www.isv.uu.se/~enberg/BK/>.
- [46] R. Enberg, Phys. Rev. D **75** (2007) 014012.
- [47] K. Golec-Biernat and A. M. Stasto, Nucl. Phys. B **668**, 345 (2003).
- [48] E. Gotsman, M. Kozlov, E. Levin, U. Maor and E. Naftali, Nucl. Phys. A **742**, 55 (2004).
- [49] J. L. Albacete, N. Armesto, J. G. Milhano, C. A. Salgado and U. A. Wiedemann, Phys. Rev. D **71**, 014003 (2005).
- [50] C. Marquet and G. Soyez, Nucl. Phys. A **760**, 208 (2005).
- [51] D. Kharzeev, Y. V. Kovchegov and K. Tuchin, Phys. Rev. D **68**, 094013 (2003).
- [52] J. Jalilian-Marian, A. Kovner, L. D. McLerran and H. Weigert, Phys. Rev. D **55**, 5414 (1997).